Semnan University

Journal of Heat and Mass Transfer Research

Journal homepage: https://jhmtr.semnan.ac.ir

ISSN: 2383-3068

Research Article

Thermal Management of Heat Sinks Equipped with Internal Cooling Mechanism: A Comparison with Advanced Heat Dissipation Techniques

Saif Ullah Khalid [a]*, Muhammad Ali Nasir [a], Mehmet Karahan [b], Muhammad Saleem Khan [c], Furqan Jamil [d]

[a] *Mechanical Engineering Department, University of Engineering and Technology, 47050 Taxila, Pakistan*

[b] *Vocational School of Technical Sciences, Bursa Uludag University, 16059 Bursa, Turkey*

[c] *Metallurgy and Materials Engineering Department, University of Engineering and Technology, Taxila 47050, Pakistan*

[d] *School of Engineering, Edith Cowan University, 270 Joondalup Drive, Joondalup, WA 6027, Australia*

ARTICLE INFO

Article history:

Received: 2025-04-29

Revised: 2025-10-05

Accepted: 2025-11-08

Keywords:

Fins;

Heat sinks;

Nanofluids,

Thermal performance augmentation;

Heat pipes.

ABSTRACT

Thermal management devices aim to remove extra heat from heat generation devices. There are numerous ways of heat rejection from the source, including active and passive cooling. The cooling techniques may be natural or forced, and the popular tools are heat pipes, heat sinks, and heat exchangers. In this piece of literature, several heat pipe and heat sink configurations are tested, including a novel internally cooled configuration using mono and hybrid nanofluids. Among heat sinks, solid finned and hollow finned configurations are mainly compared with the state-of-the-art heat pipes and thermal management systems for broader comparisons. Solid cylindrical fins are considered the baseline model, elliptical as well as semi-circular wavy are derived units, and hollow cylindrical fins are novel fin structures with important modification of water entrapment (filling ratio 50 %). Entrapped water acts as a cooling agent through heat normalization and distribution. External coolants used are water, Ethylene Glycol-based MgO nanofluids, as well as SiO_2 nanofluids, and water-based (Fe_2O_3 + TiO_2) hybrid nanofluids. Sintered copper wicked heat pipes are also diagnosed for performance evaluation with certain modifications. Tested heat pipe configurations include sintered wicked heat pipe with finless and finned arrangements, TiO_2 nanofluid, and (TiO_2 + SiO_2) hybrid nanofluid-filled heat pipes. Heat sinks proved best for higher heat loads, whereas heat pipes are an effective and sustainable option for low power range applications. Hollow cylindrical finned heat sinks possess the highest heat transfer performance factor (HTPF), followed by elliptical finned heat sinks. Based upon HTPF, hollow cylindrical finned heat sinks are preferred, whereas among heat pipes, nanofluid-filled heat pipes with fins are the best option. For water as a coolant and at 15 Watt heat input, compared to the cylindrical finned heat sinks, the elliptical, semicircular, wavy, and hollow cylindrical finned heat sinks present 20.6 %, 24.5 %, and 29.8 % higher Nusselt numbers. There is a requirement for flow rate optimization for sustainable and optimized thermal management systems.

1. Introduction

Heat transfer is a renowned process in industrial applications. In some situations, heat transfer is undesirable because it leads to energy inefficiencies, resource loss, or even system failure. On the other hand, there are many cases where efficient heat transfer is not just beneficial

* **Corresponding author.**
E-mail address: *engineersaifullahkhalid@gmail.com*

Cite this article as:

Khalid, S. U., Nasir, M. A., Karahan, M., Saleem Khan, M. and Jamil, F., 2026. Thermal Management of Heat Sinks Equipped with Internal Cooling Mechanism: A Comparison with Advanced Heat Dissipation Techniques. *Journal of Heat and Mass Transfer Research*, 13(3), pp. 335-354.

https://doi.org/10.22075/JHMTR.2025.37591.1734

but crucial to the success of a system, requiring significant investment in technologies that enhance heat transfer rates. In power generation and industrial processes, heat loss to the surroundings can significantly reduce the efficiency of energy conversion. For example, in thermal power plants, a substantial portion of the heat produced in combustion or fission processes is lost to the surroundings through exhaust gases, cooling towers, or radiation. This loss not only lowers efficiency but also requires additional fuel to compensate, increasing operational costs and contributing to environmental concerns. Latent heat storage involves storing energy through phase change (such as melting and solidification), and it's frequently used for thermal energy storage in applications like solar power, district heating, and cooling. Heat loss from these systems to the environment can reduce efficiency and increase operational costs.

There is often a requirement for smart and efficient energy transfer mechanisms, such as in a power plant, where waste heat from the condenser can be redirected to heat other parts of the plant or preheat incoming fluids. Improving heat transfer in boilers and condensers increases fuel efficiency and reduces emissions. Heat transfer is central to the efficient operation of thermal energy storage systems, especially in renewable energy applications. Solar thermal systems, for example, use heat transfer fluids to collect and store heat, which can then be used during periods when sunlight is unavailable. These systems need technologically advanced systems and well-developed mechanisms for greater efficiency and maximized yield. Optimizing heat transfer (minimizing losses or maximizing exchanges) is critical to improving system performance, reducing energy consumption, and enhancing sustainability across various industries.

Heat sinks, heat exchangers, heat pipes, and liquid absorption surfaces are effective means of heat transfer. Among thermal management devices, heat pipes and heat sinks are attaining prime importance. Thermal management devices are used in many industries, including electronics, automotive, aerospace, and manufacturing, to prevent overheating, improve energy efficiency, and extend the lifespan of components. Heat pipes are highly efficient thermal energy transfer devices that operate on the principle of phase change and convective heat transfer. Unlike conventional heat transfer methods, which rely on conduction, heat pipes leverage the latent heat of vaporization to move heat from one end of the pipe to the other. This allows heat pipes to transfer large amounts of heat with minimal temperature differences across their lengths [1].

Heat pipes are also relatively compact, lightweight, and can be designed to work passively without requiring external power sources or moving parts, ensuring reliability and low-maintenance requirements. Based upon multi-faceted benefits, heat pipes have significant applications ranging from electronic components cooling [2, 3], up to industrial equipment such as furnaces, reactors, or heat exchangers, and aerospace applications [4, 5].

Keeping in consideration the important applications of heat pipes, researchers are progressing toward performance enhancement of heat pipes using novel techniques. Various useful techniques have been adopted to increase the thermal efficiency of heat pipes, such as the use of nanofluids [6-10], utilizing self-rewetting fluids for better heat spreading properties [11-15], inclusion of wettability gradients for enhanced coolant flow [16-19], and using heat pipes at optimum inclinations [20-24], etc.

The research domain is also rapidly expanding in the field of heat sinks [25]. Several new types of heat sinks with new designs have been introduced. Researchers are continuously striving for the development of new methods and techniques for the performance enhancement of heat sinks. For example, Khan et al. [26] performed a multivariate optimization on pin-fin heat sinks for electronic cooling applications. Optimization of fin dimensions, density, spacing, and approach velocity is primarily focused on. Ahmadian-elmi et al. [27] also performed parametric optimization on a pin-fin heat sink for thermal management of electronics and concluded 17 % performance enhancement due to optimization and fin shape alteration from cylindrical to tapered. Sahel et al. [28] investigated the thermal performance of a hemispherical finned heat sink with an initial numerical study about a staggered plate finned heat sink. Comparison of results shows the advantage of using a hemispherical finned heat sink. Huang and Huang [29] studied a perforated finned heat sink and found the interesting results of perforated pins and the effect of the splitters in plate finned heat sinks. The perforation dimensions and splitter arrangement optimization were also covered in the same work. Abrofarakh and Moghadam [30] numerically investigated heat sinks equipped with novel heat transfer augmentation techniques. The hybrid nanofluid cooled heat sink was analyzed with metal foam inside the channels having corrugated walls. Three different mass fractions (0.025%, 0.05% and 0.075%) of distilled water based multi-wall carbon nano-tubes and Titanium dioxide hybrid nanofluid (MWCNTs+TiO_2) were used to analyze the effect of nanofluid concentration. The Reynolds

number during this study was 7000 to 13000. Analysis show 130 % augmentation in heat transfer using metal foam and hybrid nanofluids compared to using distilled water. The effect of metal foam porosity also impacted the results. Metal foam with 90 % porosity dissipated 9.8 % higher heat compared to one with porosity 99 %. Based on the results, important correlations between the Nusselt number and the Reynolds number were developed for all analyzed configurations. Falahat and Bahoosh [31] investigated the effect of various Alumina nanoparticle shapes on the heat transfer characteristics of a minichannel heat sink. The nanoparticle volume fractions used in this study are 0 %, 1%, 2% and 4 %. The study is performed at Reynolds numbers 114.5 and 481.5. The study concluded the achievement of the highest performance factor of 1.477 using platelet nanoparticles for volume concentration 4% and Reynolds number 114.5. Furthermore, increasing the concentration of nanoparticles and the Reynolds number has a positive impact on heat transfer enhancement, but it also elevates the pressure drop and the friction factor. Falahat et al. [32] investigated a cylindrical heat sink with helical mini-channels to analyze heat transfer and fluid flow properties. The effect of Reynolds number, mini-channel aspect ratio, and helix angle was analyzed in the context of heat transfer enhancement. Investigation shows that by increasing the Reynolds number and aspect ratio, heat transfer increases, while by increasing the helix angle, it decreases. An aspect ratio of 1.2 is observed to be optimum for maximizing the heat transfer performance factor and minimizing entropy generation. Tafarroj et al. [33] utilized an artificial neural network approach to evaluate heat transfer in a minichannel heat sink cooled by water-based Alumina nanofluid. In this regard, 60 experimental data points are used, and the best heat transfer evaluation models are developed.

The utilization of high energy materials for thermal performance augmentation of heat transfer devices is a rapidly growing domain of the current research era. Thermal performance augmentation based on applications of nanofluids, phase change materials, metal foams, and hybrid nanofluids is frequently found in the recent literature [30-37].

Esfe et al. [41] developed thermal conductivity prediction models for Ethylene Glycol-based Zinc Oxide nanofluids. Various concentrations of ZnO nanofluids were tested at different temperatures. It was analyzed that with the increase in volume concentration of nanoparticles, as well as with the increase in temperature, the thermal conductivity of nanofluids increases. Based upon extensive experimental results, thermal conductivity prediction models were proposed, which reflected good agreement with the existing models. Mohebbi et al. [42] numerically investigated the effect of water-based Al2O3 nanofluid on the heat transfer rate in various rectangular grooves. The results are computed for variable nanoparticle concentrations (0-5%) and for a wide range of Reynolds numbers (10,000-35,000). With the increase in Reynolds number as well as nano-particle concentration, heat transfer rate increases, but it also results in an increase in pressure drop. The optimized groove dimensions for enhanced heat transfer are also determined. Many researchers of the current era investigated the impact of nanofluids on heat transfer enhancement [43]. The impact of increasing nanoparticle concentration is also reported to be beneficial for heat transfer enhancement, but it also causes an increase in pressure drop and friction factor.

The cutting-edge studies include performance enhancement of heat transfer devices using the aforementioned techniques. The current study involves the manufacturing of different types of pin fins in heat sinks and the use of hybrid nanofluids and mono nanofluids as coolants for performance enhancement purposes. The novel technique of internal cooling in heat sinks was also introduced and was found to be very effective. Fins of cylindrical-pin-fin heat sinks are drilled and filled with water up to 50 % filling ratio and tested in a test rig. The performance of heat sinks is also compared with that of heat pipes. Moreover, all these combinations are presented in comparison to the state-of-the-art modern heat transfer augmentation techniques introduced by recent researchers. The comparison shows the relative pros and cons of techniques developed in this study in contrast with modern methods and techniques.

2. Methodology

2.1. Manufacturing of Heat Sinks

Heat sinks are manufactured from an aluminum square block with edge lengths of 60 mm each. The block is right-angled and machined on a 3-Axis CNC milling machine for manufacturing 41 Aluminum fins on its top face. Each fin is 25 mm long and has a cross-sectional area of 12.56 mm2. The base thickness of heat sinks is maintained at 5 mm, and extra material is removed on a wire-cut machine. The machining operation is carried out in two steps: the roughing and finishing operations. Process parameters in the first operation with the finishing allowance of 0.2 mm are 2000 spindle rpm, with 750 mm/min feed rate, and 0.5 mm

step depth. In the finishing operation, these parameters are changed to 3000, 450, and 0.25 units, respectively. This study utilizes four types of heat sinks: cylindrical finned, elliptical finned, semicircular wavy finned heat sinks, and one of the modified forms of cylindrical finned heat sinks. The modification includes drilling 25 mm deep and 2.5 mm diameter holes in cylindrical fins of the heat sink and filling with water up to 50 % filling ratio. The study also incorporates the detailed experimental results from a previous study, including four different modified forms of heat pipe (sintered copper) for a comparative study. The heat sink configurations are illustrated in Fig. 1.

2.2. Preparation of Nanofluids

Preparation of nanofluids is carried out using a two-step method. First of all, particles are stirred in a little volume of base fluid, and then the rest of the fluid is added and homogenized until the fluid is homogenized, and nanofluids are prepared. A probe type ultrasonicator is used for solution homogenization purposes. It utilizes the applications of generated ultrasonic waves. Surfactants have a very positive impact on nanofluids' stability; therefore, a small volume of surfactants, Sodium dodecyl benzene sulfate (SDBS) and polyvinyl alcohol (PVA), is added to the nanofluid suspensions for enhanced stability. The surfactants are added in the ratio of 0.10 Vol % of suspension. Table 1 presents the properties of nanofluids and associated nanoparticles.

There are various methods for the stability test of nanofluids; the simplest one is the visual testing method, in which a picture of the nanofluid is snapped and saved. This picture snapping is practiced regularly after consecutive intervals of time. At the end, all the pictures, including the last day and the first day, are compared visually to have a clear view of stability. For the achievement of better stability, some good techniques, including the addition of surfactants such as sodium dodecyl sulfate and polyvinyl, are also added to the nanofluids being prepared. Optimum stirring and sonication time also impact the stability of nanofluids.

2.3. Working Methodology

Experimentation includes a systematic procedure for the evaluation of heat dissipation characteristics of different types of heat sinks in combination with various hybrid and mono-nanofluids. Figure 2 shows the various nanofluids.

A test rig is designed for the controlled analysis at variable experimental conditions. There are several variables involved in experimentation, including the type of heat sink, the type of coolant, the flow rate of coolant, and the input heat load to the heat sink. All these combinations are tested one by one according to the established design of experiments sequence, and temperature values are recorded at the inlet and outlet of the coolant, as well as at five different positions on the surface of the heat sinks. The surface temperature of heat sinks is determined from the average of five temperatures coming from thermocouples attached to the surface of the heat sink body. There is a silicon etched foil type heater mounted at the heat sink base for heat load input, and it is insulated from the ambient. The parameters of interest are the coefficient of heat transfer, pressure drop, Nusselt number, thermal resistance, and heat transfer performance factor (HTPF). All the calculations are made at a wide range of Reynolds numbers.

2.4. Variable Control and Sensor Positions

Power is supplied to the heater through (Keysight, 6675A), the power is variable, and the voltage is varied to attain the desired power. Experimentation is performed at variable heat flux conditions. There is a proper arrangement of temperature measurement through (Extech, TP-870) thermocouples K-Type on the heat sink body, as well as at the inlet and outlet of the heat sink for the fluid. The position of thermocouples using a coordinate system, by considering one lowermost corner of the heat sink as the origin having coordinates (0,0,0), in (x,y,z) form, are presented as (2,2,5), (15,15,17.5), (30,30,60), (45,45,17.5), and (58,58,5).

The heat pipe is also provided with the thermocouples for temperature measurement. The positions of five thermocouples are at heights of 0 mm, 160 mm, 200 mm, 300 mm, and 400 mm, starting from the base of the heat pipe. For the heat sink the positions of thermocouples are presented in the form of Fig. 3.

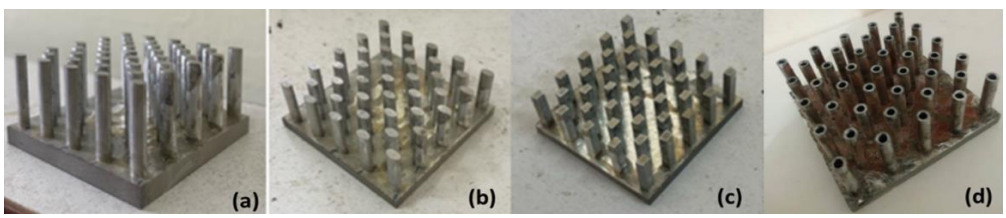

Fig. 1. (a). Cylindrical pin finned heat sink; (b) Elliptical pin finned heat sink; (c) Semicircular wavy finned heat sink; (d) Drilled modified cylindrical heat sink

Table 1. Properties of nanoparticles

S #	Nanoparticle	Sp. Heat (J/g.K)	Size (mm)	Color	Thermal Conductivity (W/m.K)	Density kg/m3	Prepared Nanofluid
1	Fe2O3	0.66	30	Dark Brown	20	5200	Water Based 0.09 Vol % (Fe2O3+TiO2) Hybrid Nanofluid
2	TiO2	0.685	30	Gray to White	8.4	4250	
3	SiO2	0.75	20	White	1.3	2650	EG & Water (1:1) Based 0.1 Vol % NF
4	MgO	0.88	20	White	50.1	3580	EG & Water (1:1) Based 0.3 Vol % NF

Fig. 2. Visual analysis of nanofluids

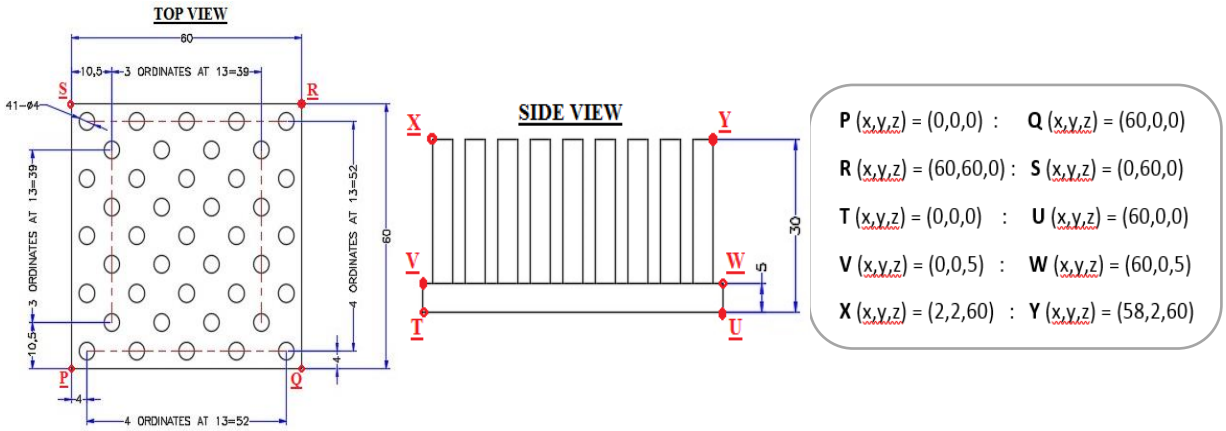

Fig. 3. Thermocouple positions on heat sink

3. Experimental Setup

The experimental setup comprises a test rig and auxiliary experimental units. The test rig is the confined Plexiglas chamber in which a heat sink is placed for testing purposes. It contains an etched foil type heater (Polisi 3D, P-1029), fitted at the base for heat input. The heat load can be varied by controlling the input power from the Keysight 6675A power supply source. Further, the heater is insulated from the ambient to ensure the entire heat flux through the heat sink. A heat sink is provided with a forced convection cooling mechanism. The system is comprised of a fluid reservoir to store the coolant, a pump for coolant transportation, a flow meter for coolant flow rate measurement, and a radiator for effective cooling of the fluid after it gains heat by passing through the heat sink. There is a proper arrangement of temperature measurement through (Extech, TP-870) thermocouples K-Type on the heat sink body, as well as at the inlet and outlet of the heat sink for the fluid. Five thermocouples are attached to the heat sink's body in this regard, one at the inlet and one at the outlet. The thermocouples are connected to the

PC through the Keysight LXI 34972A data acquisition system. A pressure transducer is used for the pressure drop measurement across the heat sink. The position of thermocouples using a coordinate system, by considering one lowermost corner of the heat sink as the origin having coordinates (0,0,0), in (x,y,z) form, are presented as (2,2,5), (15,15,17.5), (30,30,60), (45,45,17.5), and (58,58,5).

Four different heat sink configurations are experimented with in the test rig. It includes cylindrical, elliptical, and semicircular wavy finned heat sinks in addition to a hollow cylindrical finned heat sink, which is a modified form of a solid cylindrical pin finned heat sink. The coolants include hybrid and mono-nanofluids in addition to the distilled water; a total of three different nanofluids are used in this experimental analysis. The source of the nanoparticles is Nanoamor (Amorphous & Nano-structured Materials, Houston, Pennsylvania, USA). Other experimental variables include four different power levels and five different flow rates. A PC saves data through a data acquisition system for further analysis and results deduction. Figure 4 shows the experimental setup for the heat sink arrangement.

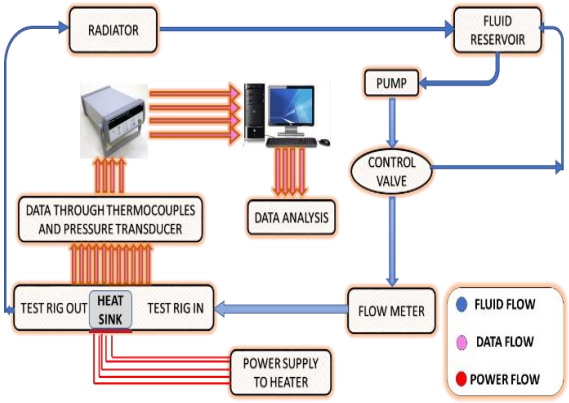

Fig. 4. Experimental setup schematic for heat sink arrangement

The experimental setup for the heat pipe comprises simple and finned sintered copper wicked heat pipes arranged in a test setup. The evaporator is wrapped with a wire-type heater at the base, is insulated with ambient, and has the model number E104257. Its composition is Nichrome (Nickel & Chromium in a 4:1 ratio) with a thermal resistance of 55 Ω/m. Glass wool and silver tape are used for insulation purposes. The condenser is left bare for forced convection. The air velocity is measured at 4 m/sec with an anemometer. A fan is used for forced convection of heat pipes; it is 12 Volt DC controlled. A flow chart has been included. A data recording system with model number LXI 34972A is used. The outer diameter (OD) and wall thickness of the heat pipe are 10 mm and 1 mm, respectively. The grade of Aluminum used is AA 6063.

Power is supplied to the heater through (Keysight, 6675A). Starting from the base, the positions of the five thermocouples are at a height of 0 mm, 160 mm, 200 mm, 300 mm, and 400 mm. A total of 30 Aluminum fins (OD: 43 mm and thickness: 0.8 mm) are equally spaced at 200 mm condenser length through interference fit. The amount of interference is 0.03 mm. Figure 5 shows the experimental setup and the position of thermocouples.

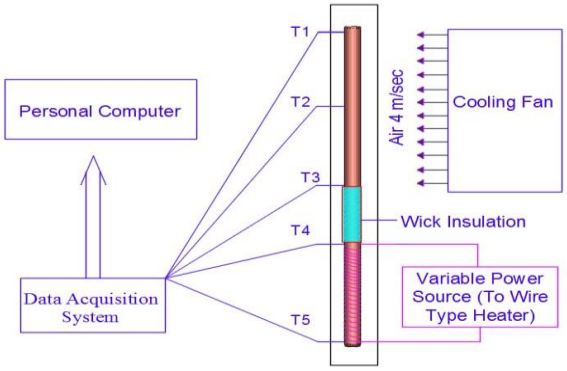

Fig. 5. Experimental setup schematic for heat pipe arrangement

As discharge is the product of velocity and flow area, the flow velocity can be computed from equation 1, as discharge and cross-sectional area are known parameters:

$$V = \frac{Q}{A} \tag{1}$$

Discharge has the units of m^3/sec, while A is the area calculated in m^2. There is a requirement for hydraulic diameter calculation for computing other thermal and hydraulic performance indicators. Hydraulic diameter is the equivalent figure for non-circular sections corresponding to circular geometries. It is provided below as the cross-sectional area to the wetted perimeter's ratio [44]:

$$Hd = \frac{4 * Ac}{P} \tag{2}$$

The Ac is not an ordinary cross-sectional area, rather it is the minimum free flow cross-sectional area and P is the wetted perimeter corresponding to the free flow cross-sectional area. It is important to calculate the Reynolds number for subsequent analysis. It is provided as [45]:

$$Re = \frac{\rho v D_h}{\mu} \tag{3}$$

where Re is the Reynolds number, ρ is the density of the working fluid, v is the velocity of the fluid, the hydraulic diameter is represented as Dh, and the dynamic viscosity is represented as μ.

Traditional working fluids possess distinct thermophysical properties, but as in the case of nanofluids, the properties can be determined from previously established relations. The density correlation is a simple average based; however, the dynamic viscosity corelation is as proposed by some researchers in the same domain [46].

$$\frac{\mu_{NF}}{\mu_{BF}} = 1 + 2.5 * \phi \quad (4)$$

The subscripts NF and BF are for nanofluid and base fluid, respectively. ϕ is the presentation of volume fraction of nanofluids. Another important factor for the performance evaluation of thermal management devices is the Nusselt number. It indicates the significance of convection relative to conduction at a solid-fluid interface during heat transfer between a solid and fluid. It is strongly affected by fluid properties because it is the direct function of the heat transfer coefficient. For forced convection based-pin finned heat sinks with cylindrical geometries, the Nusselt number is provided below as presented by researchers in literature [46, 47]:

$$Nu = \frac{Q * D_h}{K_{nf} * (T_w - T_m)} \quad (5)$$

where Nu is the Nusselt number, Q shows the heat load, Knf is the thermal conductivity of the nanofluid, Tw is the average wall temperature of the heat sink, and the mean temperature of the inlet and outlet fluid is Tm. Tm may be calculated as the average of the inlet and outlet temperatures of the cooling fluid. The thermal conductivity of the nanofluid was calculated using the empirical correlation presented below [48]:

$$\frac{k_{nf}}{k_{bf}} = \frac{[k_{np} + 2k_{bf} + 2\phi(k_{np} - k_{bf})]}{[k_{np} + 2k_{bf} - \phi(k_{np} - k_{bf})]} \quad (6)$$

This correlation is very important in explaining the thermal conductivities of nanofluids in terms of the constituting nanoparticles. Nanoparticles of TiO_2, SiO_2, and Fe_2O_3 possess thermal conductivity values of 8.4, 1.3, and 20 $W.m^{-1}K^{-1}$, respectively, and water has 0.60 $W.m^{-1}.K^{-1}$.Based on the presented correlation, thermal conductivity values of hybrid nanofluids can also be computed easily.

There is an important performance indicator in the case of thermal management devices having fluid flow applications. It is called the heat transfer performance factor (HTPF). It correlates the Nusselt number with the pressure drop value. In a few cases, a higher Nusselt number can be obtained at the expense of a higher pressure drop; therefore, HTPF would be lower than unity. While in other cases, the situation is contrasting. Always a heat transfer performance factor above unity is desired. Heat transfer performance factor is presented as follows [49]:

$$HTPF = \frac{(Nunew/Nuref)}{(\Delta Pnew/\Delta pref)^{1/3}} \quad (7)$$

Nu_{new} represents the Nusselt number achieved from a new technique, method, or design, and Nuref is the Nusselt number of a reference heat sink. Similarly, ΔP is the pressure drop for the new method or technique and for the reference heat sink. HTPF above unity shows the newly developed technique; the method of design is really effective compared to the reference case because it presents the change in heat transfer relative to the pressure drop comparison.

4. Experimental Uncertainty Analysis

It is of prime importance to analyze the experimental uncertainty in outcomes. The uncertainty of accuracy in measuring instruments leads to uncertainty in heat flux. It can be expressed as a strong function of various dependent variables, such as current (I), temperature (T), voltage (V), heat transfer area (A), and coolant mass flux (ṁ), as presented by [50]:

$$q" = f(I, V, T, A, \dot{m}) \quad (8)$$

Heat sinks are manufactured on precise CNC machines; therefore, dimensional uncertainty can be neglected. Therefore, uncertainty in heat flux can be expressed as a function of parameters affecting heat transfer rate and presented as below:

$$q" = f(I, V, T, \dot{m}) \quad (9)$$

Considering U as the uncertainty in measurements, the uncertainty correlation can be expressed as a correlation as available in recent literature [45]:

$$U_{q"} = \sqrt{U_V{}^2 + U_I{}^2 + U_T{}^2 + U_{\dot{m}}{}^2} \quad (10)$$

The above equation can be expanded in dimensionless form as presented by Babar et al. [51] and shown below:

$$\frac{U_{q"}}{q"} = \sqrt{\left(\frac{U_V}{V}\right)^2 + \left(\frac{U_I}{I}\right)^2 + \left(\frac{U_T}{T}\right)^2 + \left(\frac{U_{\dot{m}}}{\dot{m}}\right)^2} \quad (11)$$

The following table shows measuring instruments and their respective accuracy range. Based on equation 11, the fractional uncertainty in heat flux is calculated to be 0.0560 %, which is too low to be ignored. Table 2 represents a fractional uncertainty analysis.

Table 2. Fractional uncertainty analysis

Instrument Description	Measurement Range	Maximum Measurement	Accuracy Range	Maximum Uncertainty
Power Supply (Keysight 6675 A)	Voltage 0 to 110 Volts	105 Volts	± (0.04 % +0.120) V	0.162 Volts
	Current 0 to 20 Amp	0.59 Amp	± (0.1 % +0.0135) Amp	0.0141 Amp
Thermocouples (Extech TP-870)	-40 ˚C to 250˚C	76.86 ˚C	± 0.5 %	0.384 ˚C
Rotameter (Blue White F410N)	0 to 20 LPM	10 LPM	± 5 %	0.5 LPM

5. Results and Analysis

5.1. Experimental Results Validation

To validate the inferences of experimental results, current outcomes are compared with previous studies. The results are in line with the findings of recent researchers, with the minor differences due to variation in experimental conditions, dimensions of thermal management devices, coolant types, flow velocities, and experimental conditions. Values of the dimensionless Nusselt number are compared for the estimation of heat transfer characteristics associated with the current work as well as those with the existing literature, and a good agreement is observed. In general good agreement is observed between current and literature-based results [52-56] and presented in Fig. 6. To maintain parametric homogeneity, the results of various studies included in this literature review are compared with those of recent researchers on water-cooled cylindrical heat sinks.

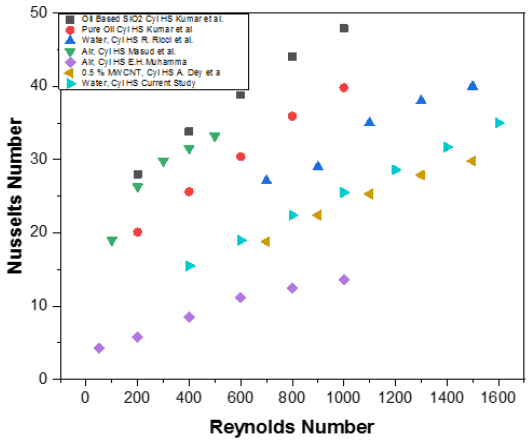

Fig. 6. Reynolds vs Nusselt number validation from literature

5.2. Average Wall Temperature Comparison

The average wall temperatures of heat sinks are compared for a relative thermal performance analysis. The average wall temperature is obtained from the mean of the temperatures obtained from thermocouples attached to the surface of the heat sink. There are various parameters that impact the wall temperature of heat sinks, such as the type of heat sink, the mass flow rate of coolant, the type of coolant, and the input power.

Average wall temperature comparison of four different variants of heat sinks is presented in Fig. 7; all the configurations are water cooled, tested at four different input powers, and five flow rate levels. Results show that the average wall temperature is highest in the case of a solid cylindrical finned heat sink, followed by an elliptical finned heat sink, and subsequently for a semicircular wavy finned heat sink; however, the lowest average wall temperature is observed for water-filled hollow cylindrical finned heat sinks. Compared to solid cylindrical finned heat sinks, elliptical finned heat sinks present 2.3 % lower average wall temperature at 2 LPM coolant flow rate and 15 Watt input heat load, the difference is 3.3 % for semicircular wavy and 4.2 % for water-filled hollow cylindrical finned heat sinks.

Further, it is observed that the average wall temperature of all types of heat sinks falls with the increase in flow rate of coolant. This decrement is fastest in the case of solid cylindrical finned heat sinks and lowest in the case of hollow cylindrical finned heat sinks, whereas elliptical finned and semicircular wavy finned heat sinks exist in between the two.

It is also observed that the difference between average wall temperatures of various heat sink types is greater at lower coolant flow rates, and the graphs converge as the coolant flow rate is increased. This is due to the most effective cooling with the enhanced heat transfer rate at higher coolant flow rates compared to lower coolant flux, especially in the case of relatively less effective heat sinks. It minimizes the difference between individual heat sink types as the coolant mass flow rate increases.

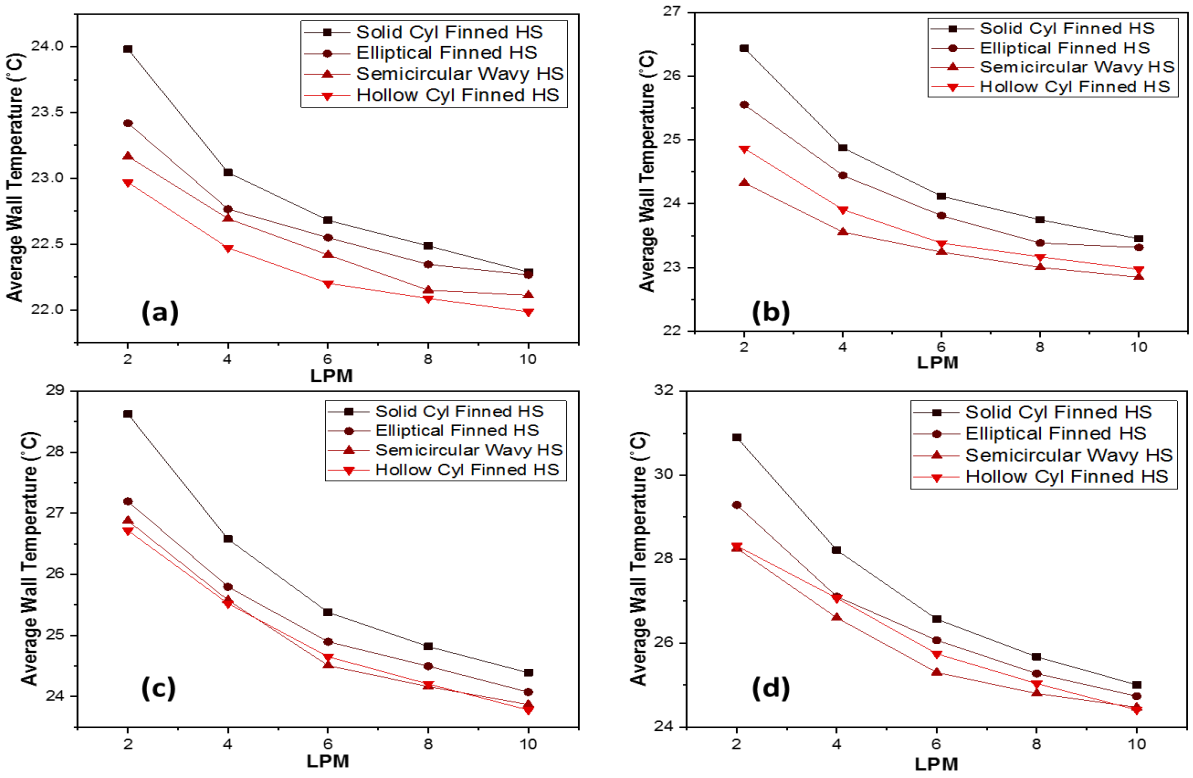

Fig. 7. LPM vs average wall temperature for water cooled heat sinks: (a) 15 W; (b) 30 W; (c) 45 W; (d) 60 W

5.3. Nusselt Number Comparison

Nusselt number is the function of Reynolds number and Prandtl number; therefore, with the increase in mass flow rate, there is also an increase in Nusselt number. However, the increase is case dependent. With the increase in input heat load, the coolant flow rate-based variation in Nusselt number is variable. At low heat loads, the increase in Nusselt number with Reynolds number is low, but at higher heat loads, the increase is more rapid. This is due to the reason that at higher heat loads, there is an enhanced heat transfer coefficient, which causes higher heat flux and therefore, higher convective heat transfer coefficients, so the Nusselt number increases. When the gradient between the coolant temperature and surface temperature of the heat sink's wall increases, it causes maximization in convective heat transfer; the rate of heat flux augmentation is not linear with the heat load. Therefore, the Nusselt number increases more rapidly with the increase in heat loads. On the other hand, the Nusselt number is also impacted by the increase in coolant flow rate. At lower heat flux values, the change in Nusselt number is less influenced by coolant flow rate compared to that at higher heat flux values. This is also due to a little temperature gradient (between coolant and surface temperature of the heat sink) at lower heat loads compared to higher heat loads. In comparison to the cylindrical finned heat sinks, the elliptical, semicircular, wavy, and hollow cylindrical finned heat sinks present 20.6 %, 24.5 %, and 29.8 % higher Nusselt numbers at 15 Watt heat load and 2 LPM coolant flow rate. The difference reduces to 8 %, 9 %, and 12.4 % at 60 Watt heat input and 10 LPM coolant flow rate, as presented in Fig. 8.

5.4. Thermal Resistances Comparison

The thermal resistance of heat sinks is inversely related to the heat transfer coefficient and their active heat transfer area. Experimental results for cylindrical finned heat sinks indicate that, in general, the thermal resistance of heat sinks is higher when water and SiO_2 are used as coolants. In contrast, thermal resistance is lower in the case of MgO and (Fe_2O_3 + TiO_2) based nanofluids. The remarkable difference is observed in the MgO case, where the lowest thermal resistance values are observed. The thermal resistance value is also flow rate dependent. It decreases remarkably with increased flow rate. The rate of change is initially higher when the flow rate increases from 2 LPM to 10 LPM, and it gradually decreases as the flow rate increases further. As higher flow rates come at the expense of weight and cost, the flow rate optimization for optimal thermal resistance in comparison to cost and weight can also be carried out using the following figure. The optimization needs the availability of application information. The available heat load and constraints. As the heat load increases, the thermal resistance of heat sinks decreases. Due to heat input augmentation, the wall temperature of heat sinks

increases, causing a greater heat transfer coefficient for an available flow rate value compared to a lower heat flux case. In this way, thermal resistance decreases continuously with the enhancement of the input heat load. As described earlier, similar to flow rate optimization, there can be converse optimization for heat sink and coolant configuration selection for an optimized input heat load for a specific application. Figure 9 presents the dynamics of a cylindrical finned heat sink with four different liquid coolant configurations, having flow rate 2 to 10 LPM, with the input heat loads 15 to 60 Watts in four equidistant stages. Thermal resistances of MgO nanofluid, (Fe_2O_3 + TiO_2) hybrid nanofluid, and SiO_2 nanofluids are 38.1 %, 15.9 %, and 2.8 % lower compared to the water-cooled cylindrical heat sink. The difference reduces to 37 %, 14.2 %, and -2.8 % at 60 watts, respectively, as shown in Fig. 9.

The thermal resistance of elliptical finned heat sinks is also inversely impacted by flow rate and input heat load values. Thermal resistance is highest for SiO_2 nanofluids and lowest for MgO nanofluids, and lies in between for water and (Fe_2O_3 + TiO_2) nanofluid for all heat load configurations, as shown in Figure 10. With the increase in flow rate, the thermal resistance of heat sinks decreases because coolant flow rate enhancement causes heat transfer augmentation and results in elevated heat transfer coefficients, which causes lower thermal resistance.

This effect is more pronounced at higher heat loads because with the enhancement in heat loads, the temperature gradient between the heat sink wall and the coolant increases, which causes greater heat transfer coefficients and subsequently a reduction in thermal resistance.

At lower heat loads, there is a greater difference in thermal resistance when different colants are compared in elliptical finned heat sinks. Thermal resistances of MgO nanofluid and (Fe_2O_3 + TiO_2) hybrid nanofluid are 36.7 % and 12.5 % lower compared to the water-cooled elliptical heat sink, respectively, whereas 14.1 % higher for SiO_2-based nanofluid; this difference changes to 36.2 %, 10.8 % and 15.4 % at 60 watts, respectively.

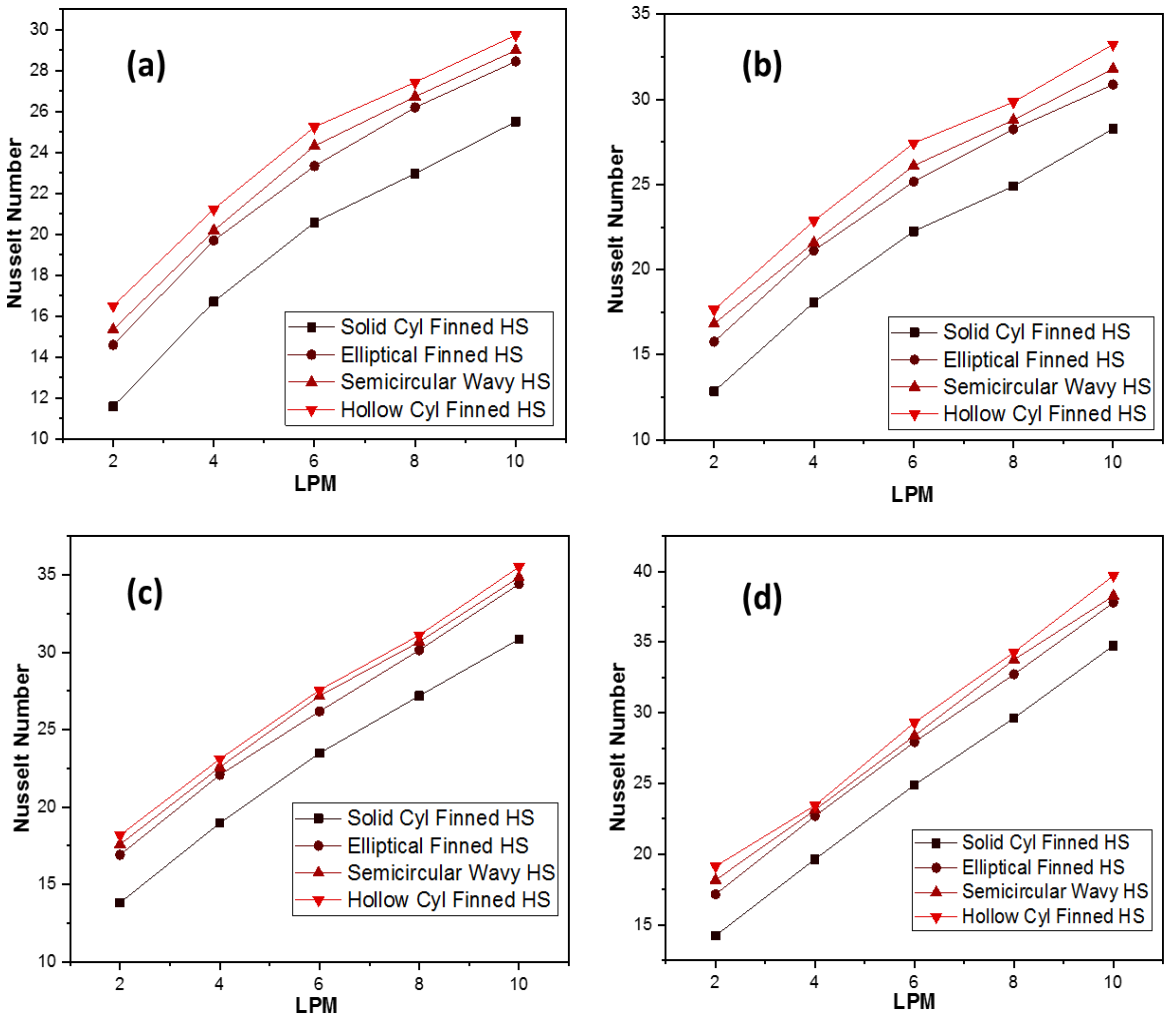

Fig. 8. LPM Vs Nusselts number: (a) 15 W; (b) 30 W; (c) 45 W; (d) 60 W

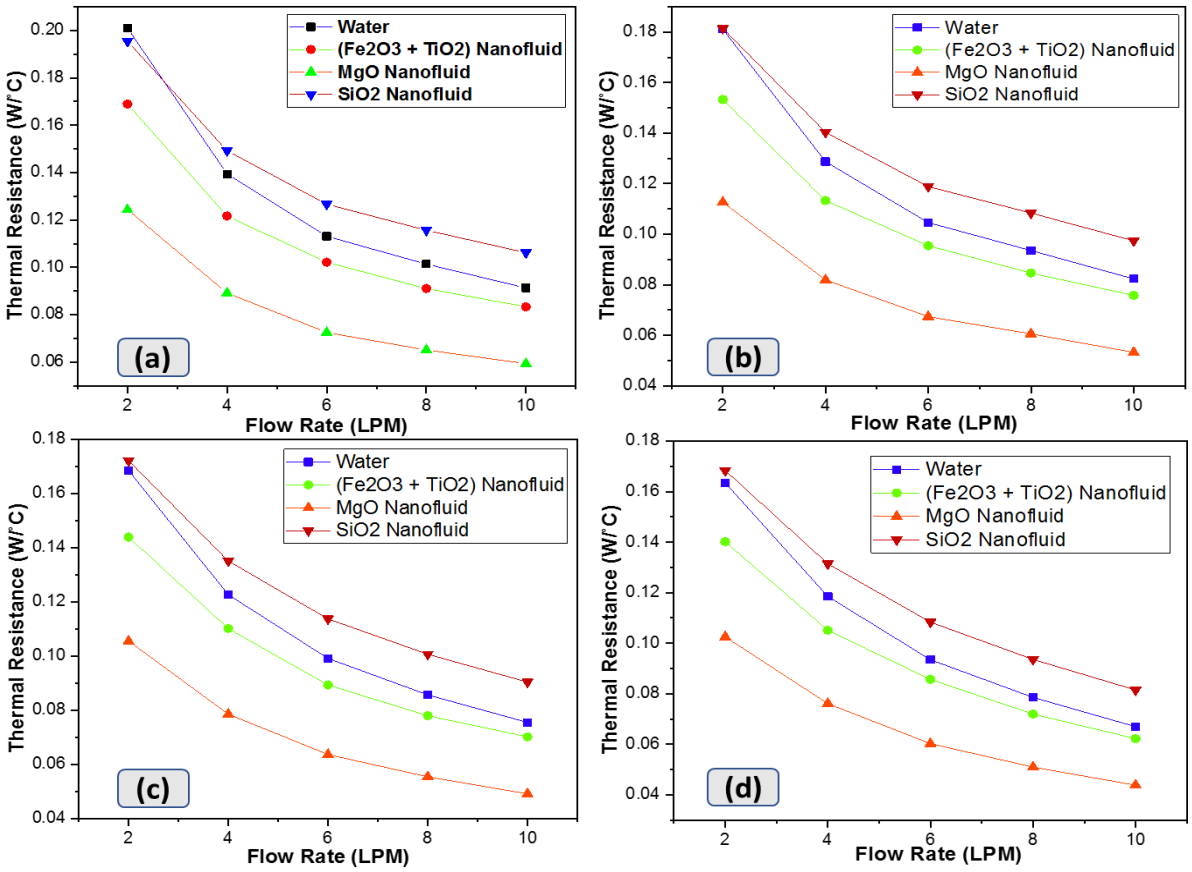

Fig. 9. LPM vs thermal resistance for cylindrical finned HS: (a) 15 W; (b) 30 W; (c) 45 W; (d) 60 W

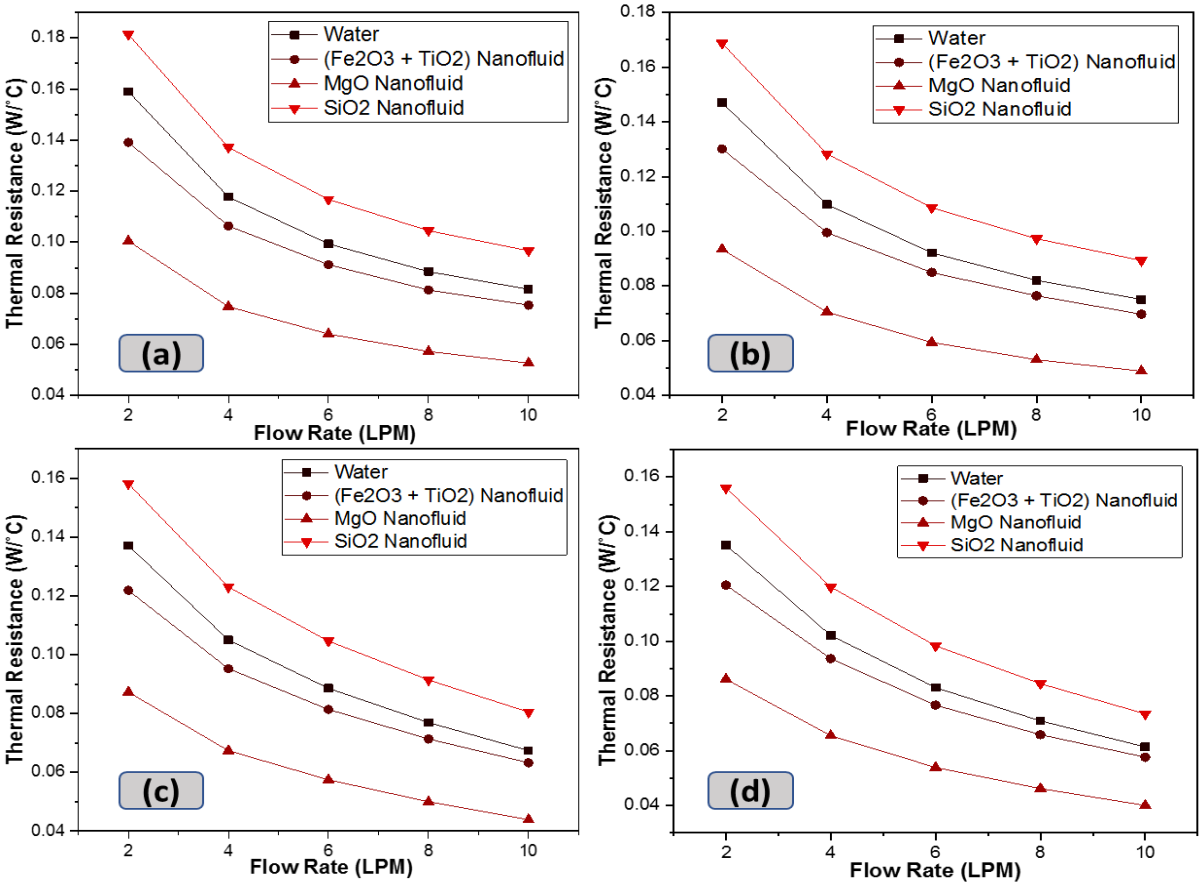

Fig. 10. LPM vs thermal resistance for elliptical finned HS: (a) 15 W; (b) 30 W; (c) 45 W; (d) 60 W

The thermal resistance of semicircular wavy finned heat sinks presents lower thermal resistance compared to elliptical finned heat sinks. There is a similar impact of flow rate and heat load enhancement as in the elliptical finned case. Both parameters impact the thermal resistance value inversely. In the case of semicircular wavy finned heat sinks, the reduction in thermal resistance is highest compared to elliptical finned and cylindrical finned heat sinks, as presented in Fig. 11. The reduction rate also increases more rapidly with the flow enhancement and heat load enhancement. It is also evident that the thermal resistance band gap for the considered configurations of heat sinks and coolants reduces with flow rate enhancement. Ideally, liquid-cooled heat sinks are best suited for higher heat load applications. The enhanced coolant flow rate results in better performance of heat sinks, but there are impediments with the higher flow rates, such as higher pumping power requirements, higher operating costs, as well as higher auxiliary system weight, etc. Therefore, the flow rate can not be set at a higher limit blindly; it needs optimization for a particular application based upon the criticality of the application, as well as heat loads, and other operating parameters. Thermal resistances of MgO nanofluid and (Fe_2O_3 + TiO_2) hybrid nanofluid are 36.1 % and 11.9 % lower compared to the water-cooled semicircular wavy finned heat sink, 15.6 % higher for SiO_2 based nanofluid. The difference reduces to 34.8 %, 10.7 %, and 16.9 % at 60 watts, respectively.

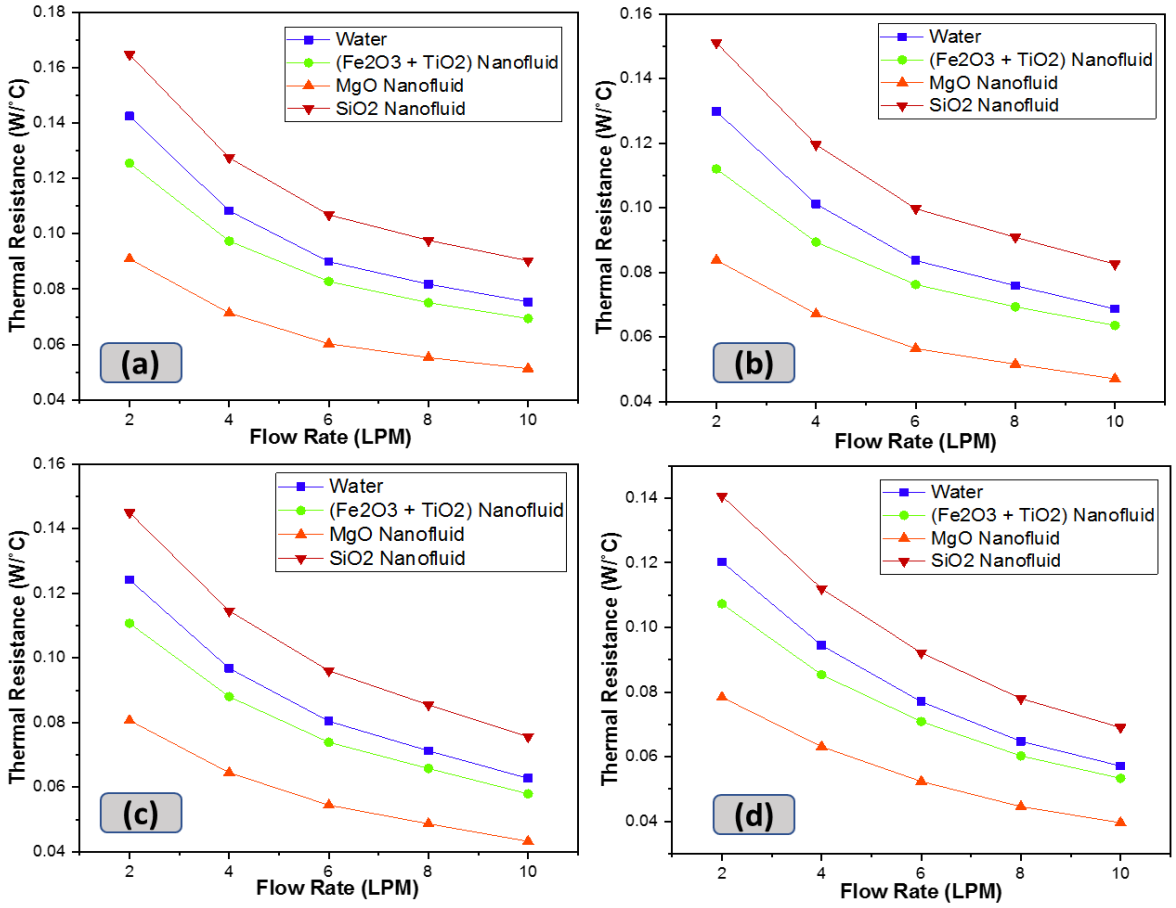

Fig. 11. LPM vs thermal resistance for semicircular wavy finned HS: (a) 15 W; (b) 30 W; (c) 45 W; (d) 60 W

5.5. Heat Transfer Performance Factor Comparison

The performance of a heat sink cannot be determined only from the heat transfer coefficient or Nusselt number value; rather, it is important to measure the heat transfer performance factor for the performance evaluation of heat sinks.

Table 3 presents the relative heat transfer performance factor. This is because the heat transfer performance factor incorporates the impact of pressure drop values compared to heat transfer enhancement for two or more heat sink configurations. The baseline configuration acts as a standard for comparison.

In the following table, a water-cooled solid cylindrical finned heat sink is considered as the baseline configuration, and three different heat sinks, including elliptical, semicircular wavy, and hollow cylindrical with water, (Fe_2O_3+TiO_2) hybrid nanofluid, MgO nanofluid, and SiO_2

nanofluid cooled configurations, are compared with the baseline model. The reason for selecting the cylindrical finned heat sink configuration as the benchmark is that it is the baseline for all other fin structures. This study considers solid cylindrical fins as the basic design and all other fins as derivatives.

However, any other configuration may also be selected as the baseline configuration. On the other hand, to keep the consistency, all combinations are compared with a water-cooled configuration (baseline model). The values above unity indicate enhancement in the heat transfer coefficient relative to the enhancement in the pressure drop when a particular configuration is compared with the baseline model.

Value unity indicates no relative change, and values below unity indicate greater impacts of pressure drop relative to heat transfer coefficients. In this way, it is concluded that generally, heat sink configurations having HTPF value greater than unity are significant and vice versa, but subjected to the special conditions, including critical applications, the heat sinks with value below unity can also be used, but they would need to afford higher pumping powers.

5.6. State of the Art Thermal Management Techniques

There are numerous heat sinks and heat pipes arrangements for thermal performance and heat transfer enhancement purposes. Several modifications have also been worked out for the performance enhancement of heat pipes and heat sinks, but there are pros and cons of each arrangement. Generally, liquid-based coolants have the advantage over modified heat sinks and heat pipes in terms of greater heat transfer capacity, lower weights, easy manufacturability, higher heat transfer coefficients, and lower operating and maintenance costs. Sometimes modifications result in thermal performance enhancement but at the cost of higher development costs, complexity, loss of reliability, and difficulty in operation and maintenance; therefore, the final decision about the significance of a modified system is subject to the relative study. In this way, a relative study is provided below for better comparison and understanding of the existing system with the advanced modified systems. The limitations associated with various state-of-the-art modified forms of heat sinks and heat pipes are presented in Table 4.

Table 3. HTPF of heat sinks compared to cylindrical solid finned heat sinks

HTPF Compared to water Cooled Solid Cylindrical Finned Heat Sink														
P (W)	**Water Based**					**Fe_2O_3+TiO_2 Based**			**MgO Based**			**SiO_2 Based**		
	LPM	**SC**	**E**	**SW**	**HC**	**SC**	**E**	**SW**	**SC**	**E**	**SW**	**SC**	**E**	**SW**
15	2	1	1.38	0.80	1.43	0.84	1.04	0.69	0.67	0.88	0.85	0.85	0.99	0.66
	4	1	1.31	0.74	1.27	0.99	1.19	0.72	0.79	1.36	0.80	1.00	1.23	0.73
	6	1	1.21	0.73	1.23	0.99	1.19	0.74	0.88	1.24	0.77	1.07	1.27	0.77
	8	1	1.19	0.82	1.19	1.02	1.20	0.84	0.96	1.21	0.81	1.09	1.29	0.88
	10	1	1.20	0.82	1.17	1.04	1.23	0.85	0.98	1.21	0.80	1.09	1.28	0.89
30	2	1	1.34	0.79	1.37	0.83	1.00	0.70	0.67	1.27	0.83	0.82	0.96	0.65
	4	1	1.30	0.73	1.26	0.98	1.18	0.73	0.80	1.33	0.78	0.98	1.22	0.72
	6	1	1.21	0.73	1.23	0.98	1.18	0.74	0.88	1.25	0.76	1.05	1.26	0.76
	8	1	1.19	0.82	1.20	1.02	1.18	0.84	0.95	1.21	0.80	1.08	1.28	0.87
	10	1	1.18	0.82	1.18	1.03	1.20	0.84	0.98	1.17	0.79	1.07	1.25	0.88
45	2	1	1.34	0.77	1.32	0.82	1.00	0.65	0.66	1.27	0.81	0.80	0.95	0.63
	4	1	1.30	0.73	1.22	0.96	1.17	0.70	0.79	1.33	0.78	0.97	1.21	0.71
	6	1	1.19	0.72	1.17	0.99	1.17	0.73	0.88	1.22	0.74	1.04	1.24	0.75
	8	1	1.16	0.80	1.14	1.01	1.16	0.81	0.95	1.18	0.78	1.06	1.25	0.85
	10	1	1.20	0.82	1.15	1.02	1.21	0.84	0.97	1.20	0.79	1.06	1.27	0.88
60	2	1	1.32	0.77	1.34	0.82	0.98	0.66	0.66	1.25	0.81	0.80	0.93	0.63
	4	1	1.29	0.72	1.19	0.97	1.15	0.70	0.79	1.33	0.77	0.96	1.20	0.70
	6	1	1.20	0.71	1.18	0.97	1.17	0.71	0.88	1.23	0.73	1.03	1.24	0.74
	8	1	1.16	0.80	1.16	1.00	1.15	0.82	0.95	1.17	0.78	1.05	1.24	0.85
	10	1	1.17	0.80	1.14	1.02	1.18	0.81	0.97	1.18	0.77	1.04	1.24	0.85

Table 4. Recent thermal management techniques

S #	Technique Used	Methodology	Limitations	Ref
1	Rotatable fins in heat sinks to adjust fluid flow and cooling capacity as per fluctuating heat load	Configuration optimization as per the variation of heat load is carried out through fin orientation adjustment. Optimized conditions for both uniform and non-uniform heat flux cases are explored.	Rotational feature is complex to incorporate and control, higher fabrication costs, and difficult with maintenance point of view	[57]
2	Integration of plate pin fins in a pin-fin heat sink oriented at an angle	The inclined plate fins incorporated among the pins of the pin finned heat sink significantly reduce the thermal resistance of the heat sink and cause higher heat flux	Flow retardation may take place, causing a higher pressure drop, making it difficult for maintenance and medium fabrication costs	[58]
3	Multilayer microjet heat sink with supercritical CO_2 to cool IGBT (Insulated Gate Bipolar Transistor) and diodes	Supercritical CO_2 is impinged in the form of microjets integrated with IGBT and diodes, which lowers the temperature of electronic components, creating a thermal management solution. Numerical studies support the experimental data, and this technique is five times more effective compared to the water cooling technique	Higher process alignment cost, maintenance is very challenging, and fabrication as well as operational cost is too high	[59]
4	Intricate heat sinks made through selective laser melting technology	Hollow lightweight and intricate heat sinks are produced with enhanced surface area and better heat spreading properties, inspired by 3D Turing patterns using selective laser beam melting technology	Higher manufacturing cost and higher pressure drop, very high maintenance cost and size limitation due to pressure drop	[60]
5	Topology optimization of heat sink based upon minimum surface lattice	The 3D printed heat sinks with minimized solid volume are the core area of this research. Hydraulic and heat transfer performance of heat sinks are enhanced using topology optimization.	Higher 3D printing cost, customized requirements of each case , high fabrication cost, and difficult to maintain	[61]
6	Nanofluid cooled micro pin finned heat sinks	A heat sink with different types of micro pin fins is cooled using nanofluids. Thermal performance augmentation is observed while using nanofluids	Limited applications only for the cases where a small amount of heat is generated, medium fabrication cost, and easy to maintain	[62]
7	Twisted pin fins in heat sinks	Heat transfer enhancement is achieved in heat sinks by twisting the pins around the major axis of the pin at different angles, optimized twist angles are also investigated	Difficult to manufacture and higher pumping power requirements, limited sizes, and higher maintenance costs	[63]
8	Cylindrical micro pin fin heat sink with hybrid nanofluid coolant	Heat sink with micro pin fins is tested using nanofluid as coolant, nanofluid based coolant enhance thermal performance of heat sinks	Compatibility with lower heat generation cases only, lower maintenance cost, and medium manufacturing cost	[64]

5.7. Relative Performance of Heat Sinks and Heat Pipes

When heat pipes and heat sinks are compared at constant heat input for relative thermal performance evaluation, it is observed that the average wall temperature of water-cooled and nanofluid-cooled heat sinks is lower than the average wall temperature of finless, finned, nanofluid-filled, and hybrid nanofluid-filled heat pipes.

Comparison of six different heat sinks and heat pipes arrangements performed in an experimental study, as shown in Fig. 12.

The baseline models are finless sintered copper wicked heat pipes and a water-cooled cylindrical finned heat sink. The derived configurations of heat pipe include finned sintered copper wicked heat pipe, TiO_2 nanofluid-filled heat pipe, and (SiO_2 + TiO_2) based hybrid nanofluid-filled heat pipes.

The derived configuration of the heat sink includes a (Fe_2O_3 + TiO_2) hybrid nanofluid cooled arrangement. All the basic and derived configurations are tested for thermal performance evaluation, which indicates that the lowest average wall temperatures are observed for the hybrid nanofluid coolant-based heat sink, whereas the highest wall temperature is observed for the finless sintered copper wicked heat pipe. Further, it is observed that heat sink systems are stable over a wide range of heat flux, whereas heat pipe systems show a greater rise in temperature with input heat load enhancement. As long as active weight and auxiliaries' weights of the system are considered, heat sink systems have more relative weights; therefore, for a decision regarding the selection of heat pipe or heat sink systems, there would be a tradeoff between quality requirement and affordable weight. The decision matrix also needs the data about the heat input range as well as the critical requirement of the heat removal process. For a less critical system with lower heat loads, heat pipes are the best choice, whereas for a system possessing higher heat loads with immediate cooling requirements, heat sinks are recommended. It is evident that heat pipes are more effective with nanofluid applications and present lower average wall temperatures, but relatively higher than the average wall temperature of liquid-cooled heat sinks.

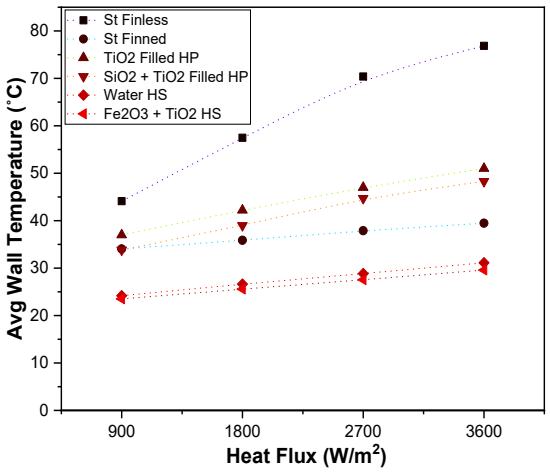

Fig. 12. Heat flux vs avgerage wall temperature for heat sinks and heat pipes [49]

6. Conclusions

There are interesting outcomes of this piece of experimental work; a few are presented below;

- Liquid-cooled thermal management devices are a prominent source of heat removal from the source generating heat as compared to air-cooled systems; however, they add extra cost and weight to the systems.
- Water-filled hollow cylindrical finned heat sinks are best suited for cooling applications, including Lithium-ion battery cooling in electric and hybrid vehicles, UAV battery cooling , and electronics and PCB cooling. This is due to the dual advantages of this configuration: higher heat flux without increasing pressure drop, and no danger of liquid coolant leakage, which is a preemptive objective in electronics to avoid burnouts due to short circuiting.
- Cylindrical, elliptical, semicircular, wavy, and hollow cylindrical finned heat sinks have been experimentally analyzed with different coolant configurations; the findings depict the privilege of using cylindrical hollow finned heat sinks, followed by semicircular wavy finned and elliptical finned heat sinks. Solid cylindrical finned heat sinks have relatively lower associated heat transfer coefficients.
- Comparison of coolants shows that the best results are achieved for MgO nanofluid, followed by Fe_2O_3 + TiO_2 hybrid nanofluids and water; however, SiO_2 nanofluid presents a lower heat transfer rate in comparison to water-based heat sinks.
- The Nusselt number of heat sinks is increasing with the increase in flow rate of coolant, but this increase is more influential with the increase in heat load. The Nusselt number of the hollow cylindrical finned heat sink is highest, followed by the semicircular wavy finned heat sink and the elliptical finned heat sink; however, the solid cylindrical finned heat sink appears to present the least priority. In comparison to the cylindrical finned heat sinks, the elliptical, semicircular, wavy and hollow cylindrical finned heat sinks present 20.6 %, 24.5 %, and 29.8 % higher Nusselt numbers at 15 Watt heat load and 2 LPM coolant flow rate (water).
- The pressure drop is highest for semicircular wavy finned heat sinks and lowest for elliptical finned heat sinks; cylindrical finned heat sinks have the same pressure drop values both in solid finned as well as hollow finned cases. Therefore, hollow cylindrical finned heat sinks have the privilege over solid cylindrical finned heat sinks in terms of enhanced thermal performance without enhancing pressure drop.
- The heat transfer performance factor of hollow cylindrical finned heat sinks is highest, while the elliptical finned heat sink is also above unity. It is found that the heat transfer performance factor of a semicircular

wavy finned heat sink is generally lowest compared to a solid cylindrical finned heat sink due to higher pressure drop values.

- The heat sinks are also compared with the state-of-the-art thermal management devices. It is observed that there are various techniques developed for thermal performance enhancement of heat transfer devices, but the modern techniques are complex, costly and subject to difficulty in operation and maintenance. Nanofluid-cooled water-filled hollow finned heat sinks are a relatively competent and simple choice.
- The average wall temperature of heat sinks is mainly heat load and coolant flow rate dependent; however, there are also impacts of coolant type and heat sink type. The lowest average wall temperature is observed in the case of a hollow cylindrical pin finned heat sink due to better heat spreading properties and an effective cooling effect due to confined liquid. Compared to solid cylindrical finned heat sinks, elliptical finned heat sinks present 2.3 % lower average wall temperature at 2 LPM coolant (water) flow rate and 15 Watt input heat load, the difference is 3.3 % for semicircular wavy and 4.2 % for water-filled hollow cylindrical finned heat sinks.
- The relative thermal performance of water-filled hollow cylindrical finned heat sinks is far above all other types of heat sinks, experimentally analyzed in this piece of literature.
- Flow rate optimization is the preemptive requirement for a liquid-cooled heat sink-based thermal management system. It would yield optimized weight and enhanced heat transfer performance factor for the system.
- There are numerous practical applications associated with current work, ranging from commercial to industrial applications. The sedimentation and agglomeration problem associated with nanofluids is well-renowned and has been worked on by many researchers. Although many researchers presented interesting methods for stability enhancement, there is still a requirement for long term stability achievement methodologies. Use of a mechanical idler stirrer or dummy pump is recommended in this regard, which may act as a source of agitation.

7. Future Recommendations

The research can further be extended to the new domains of artificial intelligence (such as Simulated Annealing) and machine learning-based control systems (Multilayer Neural Network and Fuzzy-based models). The purpose of utilizing intelligent control systems is optimization of coolant flow rate to minimize the pumping power and optimum cooling as per heat extraction rate needs. Heat sinks manufacturing using new methods and techniques may also be explored.

Nomenclature

A	Area [m^2]
D	Diameter [m]
h	Heat transfer coefficient [W/m^2K]
k	Thermal conductivity [W/mK]
L	Length [m]
Nu	Nusselt number
P	Pressure [bar]
Q	Heat transfer [W]
Re	Reynolds number
T	Temperature [°C]
V	Velocity [m/s]
W	Applied heat load [W]

Greek symbols

ρ	Density [kg/m^3]
μ	Dynamic viscosity []
ϕ	Concentration

Abbreviations

Al	Aluminum
Fd	Finned
Fs	Finless
E	Elliptical
Fe_2O_3	Iron Oxide
HC	Hollow Cylindrical
Hp	Heat pipe
HTPF	Heat transfer performance factor
HS	Heat sinks
LPM	Litre per minute
MgO	Magnesium Oxide
PCM	Phase Change Material
Reg	Regression
SiO_2	Silicon Oxide
SC	Solid Cylindrical
St	Sintered
SW	Semi-circular Wavy
TiO_2	Titanium Oxide

Scripts

Nf	Nanofluid
Np	Nanoparticles

Funding Statement

This research did not receive any specific grant from funding agencies in the public, commercial, or not-for-profit sectors.

Conflicts of Interest

The author declares that there is no conflict of interest regarding the publication of this article.

Authors Contribution Statement

Saif Ullah Khalid: Conceptualization, Data Curation, Formal Analysis, Investigation, Methodology.

Muhammad Ali Nasir: Project Administration, Supervision, Methodology.

Mehmet Karahan: Validation, Visualization, Resources.

Muhammad Saleem Khan: Writing- Original Draft.

Furqan Jamil: Writing-Review & Editing.

References

[1] Nazari, M. A., Ghasempour, R., Ahmadi, M. H., Heydarian, G., Shafii, M. B., 2018. Experimental investigation of graphene oxide nanofluid on heat transfer enhancement of pulsating heat pipe. *International Communications in Heat and Mass Transfer*, 91, pp. 90–94.

[2] Chen, X., Ye, H., Fan, X., Ren, T., Zhang, G., 2016. A review of small heat pipes for electronics. *Applied Thermal Engineering*, 96, pp. 1–17.

[3] Belmonte, J. F., Molina, A. E., 2015. Fins with a prescribed temperature at the tip: Efficiency and effectiveness expressions. *Applied Thermal Engineering*, 91, pp. 447–455.

[4] Mashaei, P. R., Shahryari, M., Fazeli, H., Hosseinalipour, S. M., 2016. Numerical simulation of nanofluid application in a horizontal mesh heat pipe with multiple heat sources: A smart fluid for high efficiency thermal system. *Applied Thermal Engineering*, 100, pp. 1016–1030.

[5] Ömür, C., Uygur, A. B., Horuz, İ., Işık, H. G., Ayan, S., Konar, M., 2018. Incorporation of manufacturing constraints into an algorithm for the determination of maximum heat transport capacity of extruded axially grooved heat pipes. *International Journal of Thermal Sciences*, 123, pp. 181–190.

[6] Wang, G., Song, B., Liu, Z., 2010. Operation characteristics of cylindrical miniature grooved heat pipe using aqueous CuO nanofluids. *Experimental Thermal and Fluid Science*, 34(8), pp. 1415–1421.

[7] Putra, N., Septiadi, W. N., Rahman, H., Irwansyah, R., 2012. Thermal performance of screen mesh wick heat pipes with nanofluids. *Experimental Thermal and Fluid Science*, 40, pp. 10–17.

[8] Kang, S. W., Wei, W. C., Tsai, S. H., Huang, C. C., 2009. Experimental investigation of nanofluids on sintered heat pipe thermal performance. *Applied Thermal Engineering*, 29(5–6), pp. 973–979.

[9] Liu, Z. H., Li, Y. Y., 2012. A new frontier of nanofluid research: Application of nanofluids in heat pipes. *International Journal of Heat and Mass Transfer*, 55(23–24), pp. 6786–6797.

[10] Buschmann, M. H., 2013. Nanofluids in thermosyphons and heat pipes: Overview of recent experiments and modelling approaches. *International Journal of Thermal Sciences*, 72, pp. 1–17.

[11] Ghanbarpour, M., Nikkam, N., Khodabandeh, R., Toprak, M.S., Muhammed, M., 2015. Thermal performance of screen mesh heat pipe with Al_2O_3 nanofluid. *Experimental Thermal and Fluid Science*, 66, pp. 213–220.

[12] Siavashi, M., Reza, H., Bahrami, T., Aminian, E., Saffari, H., 2019. Numerical analysis on forced convection enhancement in an annulus using porous ribs and nanoparticle addition to base fluid, *Journal of Central South University*, 26, pp. 1089-1998.

[13] Hu, Y., Huang, K., Huang, J., 2018. A review of boiling heat transfer and heat pipes behaviour with self-rewetting fluids. *International Journal of Heat and Mass Transfer*, 121, pp. 107–118.

[14] Lefèvre, F., Rullière, R., Pandraud, G., Lallemand, M., 2008. Prediction of the temperature field in flat plate heat pipes with micro-grooves - Experimental validation. *International Journal of Heat and Mass Transfer*, 51, pp. 4083-4094.

[15] Boubaker, R., Harmand, S., Ouenzerfi, S., 2019. Effect of self-rewetting fluids on the liquid/vapor phase change in a porous media of two-phase heat transfer devices. *International Journal of Heat and Mass Transfer*, 136, pp. 655–663.

[16] Cheng, J., Wang, G., Zhang, Y., Pi, P., Xu, S., 2017. Enhancement of capillary and thermal performance of grooved copper heat pipe by gradient wettability surface. *International Journal of Heat and Mass Transfer*, 107, pp. 586–591.

[17] Singh, M., Varma, N., Kondaraju, S., Singh, S., 2018. Enhanced thermal performance of micro heat pipes through optimization of wettability gradient. *Applied Thermal Engineering*, 143, pp. 350–357.

[18] Hu, Y., Cheng, J., Zhang, W., Shirakashi, R., Wang, S., 2013. Thermal performance enhancement of grooved heat pipes with inner surface treatment. *International Journal of Heat and Mass Transfer*, 67, pp. 416–419.

[19] Savino, R., Di Paola, R., Cecere, A., Fortezza, R., 2010. Self-rewetting heat transfer fluids and nanobrines for space heat pipes. *Acta Astronautica*, 67, pp. 1030–1037.

[20] Gurses, A. C., Cannistraro, C., Tezcan, L., 1991. The inclination effect on the performance of water-filled heat pipes. *Renewable Energy*, 1(5–6), pp. 667–674.

[21] Sadeghinezhad, E., et al., 2016. Experimental investigation of the effect of graphene nanofluids on heat pipe thermal performance. *Applied Thermal Engineering*, 100, pp. 775–787.

[22] Zhihu, X., Wei, Q., 2014. Experimental study on effect of inclination angles to ammonia pulsating heat pipe. *Chinese Journal of Aeronautics*, 27(5), pp. 1122–1127.

[23] Vijayakumar, M., Navaneethakrishnan, P., Kumaresan, G., Kamatchi, R., 2017. A study on heat transfer characteristics of inclined copper sintered wick heat pipe using surfactant-free CuO and Al_2O_3 nanofluids. *Journal of the Taiwan Institute of Chemical Engineers*, 81, pp. 190–198.

[24] Wang, P. Y., Chen, X. J., Liu, Z. H., Liu, Y. P., 2012. Application of nanofluid in an inclined mesh wicked heat pipe. *Thermochimica Acta*, 539, pp. 100–108.

[25] Hu, X., Yuan, W., Zhang, X., Gong, X., Shuai, Y., He, S., 2025. Comparative studies on thermal management performance of PCM-based heat sinks filled with various height structured porous materials. *Applied Thermal Engineering*, 263, p. 125376.

[26] Khan, W. A., Culham, J. R., Yovanovich, M. M., 2008. Modeling of cylindrical pin-fin heat sinks for electronic packaging. *IEEE Transactions on Components and Packaging Technologies*, 31(3), pp. 536–545.

[27] Ahmadian-Elmi, M., Mashayekhi, A., Nourazar, S. S., Vafai, K., 2021. A comprehensive study on parametric optimization of the pin-fin heat sink to improve its thermal and hydraulic characteristics. *International Journal of Heat and Mass Transfer*, 180, p. 121797.

[28] Sahel, D., Bellahcene, L., Yousfi, A., Subasi, A., 2021. Numerical investigation and optimization of a heat sink having hemispherical pin fins. *International Communications in Heat and Mass Transfer*, 122, p. 105133.

[29] Huang, C., Huang, Y., 2021. An optimum design problem in estimating the shape of perforated pins and splitters in a plate-pin-fin heat sink. *International Journal of Thermal Sciences*, 170, p. 107096.

[30] Abrofarakh, M., Moghadam, H., 2023. Numerical study on thermo-hydraulic performances of hybrid nanofluids flowing through a corrugated channel with metal foam. *Journal of Heat and Mass Transfer Research*, 10, pp. 147–158.

[31] Falahat, A., Bahoosh, R., 2022. The effect of nanoparticle shape on hydrothermal performance and entropy generation of boehmite alumina nanofluid in a cylindrical heat sink with helical minichannels. *Journal of Heat and Mass Transfer Research*, 9, pp. 85–98.

[32] Falahat, A., Bahoosh, R., Noghrehabadi, A., 2018. A numerical investigation of heat transfer and pressure drop in a novel cylindrical heat sink with helical minichannels. *Journal of Heat and Mass Transfer Research*, 5, pp. 11–26.

[33] Tafarroj, M.M., Mousavi Ajarostaghi, S.S., Ho, C.J., Yan, W.M., 2024. Artificial neural network approaches for predicting the heat transfer in a mini-channel heatsink with alumina/water nanofluid. *Journal of Heat and Mass Transfer Research*, 11(21), pp. 75–88.

[34] Li, Y., Gong, L., Xu, M., Joshi, Y., 2019. Hydraulic and thermal performances of metal foam and pin fin. *Applied Thermal Engineering*, 166, p. 114665.

[35] Samudre, P., Vasu, S., 2022. Thermal performance enhancement in open-pore metal foam and foam-fin heat sinks for electronics cooling. *Applied Thermal Engineering*, 205, p. 117885.

[36] Ullah, S., Hasnain, S., Muhammad, H., Bano, S., Ali, M., Abbas, N., 2022. Experimental investigation of aluminum fins on relative thermal performance of sintered copper wicked and grooved heat pipes. *Progress in Nuclear Energy*, 152, p. 104374.

[37] Rehman, T., 2018. Experimental investigation on paraffin wax integrated with copper foam based heat sinks for electronic components thermal cooling. *International Communications in Heat and Mass Transfer*, 98, pp. 155–162.

[38] Abdelaziz, A. H., El-Maghlany, W. M., El-Din, A. A., Alnakeeb, M. A., 2022. Mixed convection heat transfer utilizing nanofluids, ionic nanofluids, and hybrid nanofluids in a horizontal tube. *Alexandria Engineering Journal*, 61(12), pp. 9495–9508.

[39] Bozorgan, N., Shafahi, M., 2017. Analysis of gasketed-plate heat exchanger performance using nanofluid. *Journal of Heat and Mass Transfer Research*, 4, pp. 65–72.

[40] Dibaei, M. H., Kargarsharifabad, H., 2017. New achievements in Fe_3O_4 nanofluid fully developed forced convection heat transfer under the effect of a magnetic field: An experimental study. *Journal of Heat and Mass Transfer Research*, 4, pp. 1–12.

[41] Esfe, M. H., Saedodin, S., 2014. Experimental investigation and proposed correlations for temperature-dependent thermal conductivity enhancement of ethylene glycol based nanofluid containing ZnO nanoparticles. *Journal of Heat and Mass Transfer Research*, 1(1), pp. 47–54.

[42] Mohebbi, K., Rafee, R., Talebi, F., 2015. Effects of the rectangular groove dimensions on the thermal features of the turbulent Al_2O_3-water nanofluid flow in the grooved tubes. *Journal of Heat and Mass Transfer Research*, 2, pp. 59–70.

[43] Rezaei, A., Baniamerian, Z., 2021. Hydro-thermal performance evaluation of nanofluids flow in double pipe heat exchanger: Effects of inner pipe cross section, circular or cam-shaped. *Journal of Heat and Mass Transfer Research*, 8, pp. 283–299.

[44] Nilpueng, K., et al., 2021. Effect of pin fin configuration on thermal performance of plate pin fin heat sinks. *Case Studies in Thermal Engineering*, 27, p. 101269.

[45] Babar, H., Wu, H., Zhang, W., 2023. Investigating the performance of conventional and hydrophobic surface heat sink in managing thermal challenges of high heat generating components. *International Journal of Heat and Mass Transfer*, 216, p. 124604.

[46] Raihan, A., Ali, I., Salam, B., 2020. A review on nanofluid: Preparation, stability, thermophysical properties, heat transfer characteristics and application. *SN Applied Sciences*, 2(10), pp. 1–17.

[47] Jeng, T., Tzeng, S., 2020. Effects of passage divider and packed brass beads on heat transfer characteristic of the pin-fin heat sink by water cooling. *Heat and Mass Transfer*, 1, pp. 1429–1441.

[48] Kumar, T. A., Pradyumna, G., Jahar, S., 2012. Investigation of thermal conductivity and viscosity of nanofluids. *Journal of Environmental Research And Development*, 7(2), pp. 768-777.

[49] Ullah, S., Nasir, M.A., Aqeel, M., Khan, M.S., Hanna, E.G., Ali, H.M., 2025. Thermal and hydraulic performance evaluation of heat sinks using nanofluids and innovative vortex generating fins. *Journal of Thermal Analysis and Calorimetry*, 150, pp. 4405–4427.

[50] Khalid, S. U., Hasnain, S., Ali, H. M., Bano, S., 2022. Experimental investigation of thermal performance characteristics of sintered copper wicked and grooved heat pipes: A comparative study. *Journal of Central South University*, 28, pp. 3507–3520.

[51] Shah, T.R., Ali, H.M., Zhou, C., Babar, H., Janjua, M.N., Doranehgard, M.H., Hussain, A., Sajjad, U., Wang, C.C., Sultan, M., 2022. Potential evaluation of water-based ferric oxide (Fe_2O_3-water) nanocoolant: An experimental study. *Energy*, 246, pp. 246.

[52] Dey, A., Ahmed, Z. U., Alam, R., 2022. Thermal and exergy analysis of pin-finned heatsinks for nanofluid cooled high concentrated photovoltaic thermal (HCPV/T) hybrid systems. *Energy Conversion and Management: X*, 16, p. 100324.

[53] Muhammad, E. H., 2015. A comparison of the heat transfer performance of a hexagonal pin fin with other types of pin fin heat sinks. *Thermal Science and Engineering Progress*, 4(9), pp. 1781–1789.

[54] Behnia, M., Copeland, D., Soodphakdee, D., 1998. A comparison of heat sink geometries

for laminar forced convection: Numerical simulation of periodically developed flow. IEEE, Intersociety Conference on Thermal and Thermomechanical Phenomena in Electronic Systems (ITHERM), Sheraton Seattle Hotel and Towers Seattle, Washington, USA May 27-30,1998.

[55] Ricci, R., Montelpare, S., 2006. An experimental IR thermographic method for the evaluation of the heat transfer coefficient of liquid-cooled short pin fins arranged in line. *Experimental Thermal and Fluid Science*, 30, pp. 381–391.

[56] Kumar, S., Sharma, M., Bala, A., Kumar, A., Maithani, R., Sharma, S., Alam, T., Gupta, N.K., Sharifpur, M., 2022. Enhanced heat transfer using oil-based nanofluid flow through conduits: A review. *Energies*, 15.

[57] Hu, Q., Chen, W., Men, Z., Liu, S., 2025. Performance evaluation and experimental verification of optimizing fin angles in adjustable-configuration heat sinks. *Applied Thermal Engineering*, 258, p. 124635.

[58] Ismail, M., Manasrah, A., Masoud, A., Abedalaziz, M., 2024. Hydrothermal performance of a heat sink using plate-fins: Experimental and numerical investigations. *International Journal of Thermofluids*, 23, p. 100813.

[59] Ismail, M., 2024. Experimental and numerical analysis of heat sink using various patterns of cylindrical pin-fins. *International Journal of Thermofluids*, 23, p. 100737.

[60] Zhong, S., Li, J., Hu, K., Wang, X., Yang, L., 2024. Experimental and numerical investigation of heat sinks constructed by anisotropic 3-D Turing patterns. *International Journal of Heat and Mass Transfer*, 233, p. 126024.

[61] Modrek, M., Khan, K. A., Hassan, M. I., Al-Rub, K. A., 2024. Multi-objective topology optimization and numerical investigation of heat sinks based on triply periodic minimal surface lattices. *Case Studies in Thermal Engineering*, 63, p. 105255.

[62] Ben, N., et al., 2024. Eulerian-Lagrangian numerical investigation of the fluid flow properties and heat transfer of a nanofluid-cooled micro pin-fin heat sink. *Journal of the Taiwan Institute of Chemical Engineers*, 164, p. 105674.

[63] Mimi, A., Abdelaziz, G. B., Sharshir, S. W., El-Said, E. M. S., 2024. Orientation effects on mixed convective performance of twisted pin fin heat sink: Experimental investigation. *Applied Thermal Engineering*, 250, p. 123490.

[64] Basem, A., Abdeldayem, M., Jasim, D. J., Nabi, H., 2024. Exploring the efficiency of employing Fe_3O_4-MWCNT nanofluids in a heat sink equipped with circular micro pin-fins. *International Journal of Thermofluids*, 24, p. 100928.